Mingzhan Xue,[1] Martin O. Weickert,[1,2] Sheharyar Qureshi,[1,2]
Ngianga-Bakwin Kandala,[3] Attia Anwar,[1] Molly Waldron,[1] Alaa Shafie,[1]
David Messenger,[4] Mark Fowler,[4] Gail Jenkins,[4] Naila Rabbani,[5] and Paul J. Thornalley[1,5]

Improved Glycemic Control and Vascular Function in Overweight and Obese Subjects by Glyoxalase 1 Inducer Formulation

Diabetes 2016;65:2282–2294 | DOI: 10.2337/db16-0153

OBESITY STUDIES

Risk of insulin resistance, impaired glycemic control, and cardiovascular disease is excessive in overweight and obese populations. We hypothesized that increasing expression of glyoxalase 1 (Glo1)—an enzyme that catalyzes the metabolism of reactive metabolite and glycating agent methylglyoxal—may improve metabolic and vascular health. Dietary bioactive compounds were screened for Glo1 inducer activity in a functional reporter assay, hits were confirmed in cell culture, and an optimized Glo1 inducer formulation was evaluated in a randomized, placebo-controlled crossover clinical trial in 29 overweight and obese subjects. We found *trans*-resveratrol (tRES) and hesperetin (HESP), at concentrations achieved clinically, synergized to increase Glo1 expression. In highly overweight subjects (BMI >27.5 kg/m^2), tRES-HESP coformulation increased expression and activity of Glo1 (27%, $P < 0.05$) and decreased plasma methylglyoxal (−37%, $P < 0.05$) and total body methylglyoxal-protein glycation (−14%, $P < 0.01$). It decreased fasting and postprandial plasma glucose (−5%, $P < 0.01$, and −8%, $P < 0.03$, respectively), increased oral glucose insulin sensitivity index (42 mL · min^{-1} · m^{-2}, $P < 0.02$), and improved arterial dilatation Δbrachial artery flow-mediated dilatation/Δdilation response to glyceryl nitrate (95% CI 0.13–2.11). In all subjects, it decreased vascular inflammation marker soluble intercellular adhesion molecule-1 (−10%, $P < 0.01$). In previous clinical evaluations, tRES and HESP individually were ineffective. tRES-HESP coformulation could be a suitable treatment for improved metabolic and vascular health in overweight and obese populations.

Increasing overweight and obese populations are driving a global epidemic of type 2 diabetes and cardiovascular disease in Westernized countries. Glyoxalase 1 (Glo1) was linked to clinical obesity through association with measures of fat deposition and Glo1 deficiency identified as a driver of cardiovascular disease in a large integrative genomics study (1,2). It is currently unaddressed by therapeutic agents. Experimental studies found that overexpression of Glo1 in mice suppressed inflammation and body weight gain in overfeeding models of obesity and prevented vascular disease in diabetes (3).

Glo1 is part of the glyoxalase metabolic pathway, which consists of two enzymes, Glo1 and Glo2, and a catalytic amount of reduced glutathione (GSH) in the cytoplasm of cells (Fig. 1*A*). The major function of the glyoxalase pathway is detoxification of the reactive dicarbonyl metabolite, methylglyoxal, converting it to D-lactate. Methylglyoxal is a highly potent glycating agent of protein that forms the quantitatively major advanced glycation end product, hydroimidazolone MG-H1, linked to protein inactivation and cell dysfunction (4,5) (Fig. 1*B*). Degradation of methylglyoxal-modified proteins releases MG-H1 free adduct from tissues for urinary excretion (4). The steady-state level of protein MG-H1 is maintained at low tolerable levels by Glo1 (3).

Abnormally high methylglyoxal concentration, dicarbonyl stress, is a common characteristic of obesity and type 2 diabetes. It is severe in diabetes, driven by increased flux of

[1]Clinical Sciences Research Laboratories, Warwick Medical School, University of Warwick, University Hospital, Coventry, U.K.
[2]Warwickshire Institute for the Study of Diabetes, Endocrinology and Metabolism, University Hospitals of Coventry and Warwickshire National Health Service Trust, Coventry, U.K.
[3]Division of Health Sciences, Warwick Medical School, University of Warwick, Coventry, U.K.
[4]Unilever Research & Development Colworth, Bedford, U.K.
[5]Warwick Systems Biology Centre, University of Warwick, Coventry, U.K.
Corresponding author: Paul J. Thornalley, p.j.thornalley@warwick.ac.uk.

Received 2 February 2016 and accepted 27 April 2016.
Clinical trial reg. no. NCT02095873, clinicaltrials.gov.
This article contains Supplementary Data online at http://diabetes.diabetesjournals.org/lookup/suppl/doi:10.2337/db16-0153/-/DC1.

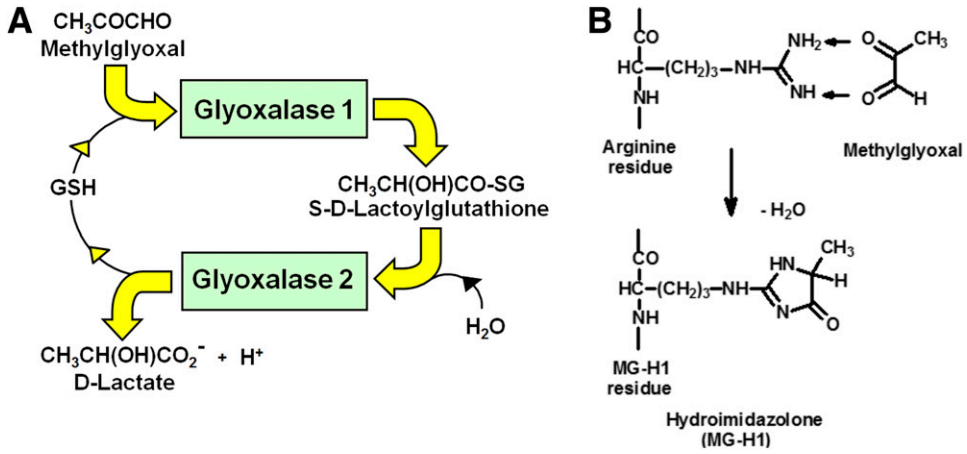

Figure 1—Glyoxalase pathway and protein glycation by methylglyoxal. *A*: Metabolism of methylglyoxal by the glyoxalase system. *B*: Formation of hydroimidazolone MG-H1 from arginine residues in protein.

methylglyoxal formation and decreased Glo1 activity at sites of vascular complications. Methylglyoxal is formed mainly by the nonenzymatic degradation of triosephosphate intermediates of glycolysis—a minor "leak" of ~0.05% triosephosphate flux. In obesity, dicarbonyl stress is mild and triosephosphate flux is increased by glyceroneogenesis in adipose tissue–liver cycling of triglycerides and free fatty acids. Increased methylglyoxal protein modification in dicarbonyl stress is implicated as a mediator of impaired metabolic and vascular health in obesity and diabetes (3).

An effective strategy to counter dicarbonyl stress is to increase expression of Glo1 (6). We described a functional regulatory antioxidant response element (ARE) in human GLO1 with basal and inducible expression upregulated by transcriptional factor nuclear factor E2-related factor 2 (Nrf2). Recent advances in Nrf2 regulation suggested that potent induction of Glo1 expression could be achieved by a synergistic combination of Nrf2 activators addressing different regulatory features (7,8). In this study, we sought to screen dietary bioactive compounds for Glo1 inducer activity in a functional reporter assay, confirm hits in cell culture, and evaluate an optimized Glo1 inducer formulation in a randomized, placebo-controlled crossover clinical trial for improved metabolic and vascular health in overweight and obese subjects.

RESEARCH DESIGN AND METHODS

Screening of Glo1 Inducers Using GLO1-ARE and Related Stable Transfectant Reporter Cell Lines

Stable transfectant luciferase reporter cell lines with ARE transcriptional regulatory elements were developed from human HepG2 cells, as described for quinone reductase ARE (7), incorporating regulatory elements: GLO1-ARE or functionally inactive mutant as negative control (ARE-1 and ARE1m in previous work) (6). Stable transfectant cell lines were incubated with and without bioactive compounds (0.625–20.0 μmol/L) for 6 h. Luciferase activity was then determined in cell lysates, with correction for blank response, and normalized to the highest effect (100%) achieved with 10 μmol/L *trans*-resveratrol (tRES) (6). Nrf2-dependent transcriptional response was verified by small interfering RNA silencing of Nrf2. Cytotoxicity was assessed after 24 h exposure by the MTT [3-(4,5-dimethylthiazol-2-yl)-2,5-diphenyltetrazolium bromide] method (9). Screening hit criteria were as follows: increased transcriptional response at ≤5 μmol/L without significant cytotoxicity to human aortal endothelial cells (HAECs) and BJ human foreskin fibroblasts in primary culture. Dietary bioactive compound selection criteria were ability to activate Nrf2 at concentrations achieved or likely achievable at tolerable doses clinically and/or decrease glycation and/or toxicity by methylglyoxal or similar compounds.

ARE-Linked Gene and Other Cell Metabolism and Functional Marker Gene Expression by Digital mRNA Profiling and Immunoblotting

HAECs, BJ fibroblasts, and HepG2 cells (5×10^5 cells/well) were seeded on sixwell plates in relevant medium and cultured overnight at 37°C under 5% CO_2/air. Cells were treated with and without 5 μmol/L tRES, 5 μmol/L hesperetin (HESP), and 5 μmol/L tRES plus HESP combined or vehicle (0.002% dimethylsulfoxide) and cultured further for up to 48 h. At the time points indicated, mRNA was extracted and analyzed by the NanoString nCounter method (10). Immunoblotting was performed as previously described (6).

Clinical Study

A randomized, double-blind, placebo-controlled crossover study of optimized Glo1 inducer was performed in 32 overweight and obese healthy subjects (Healthy Ageing through functional food [HATFF]). The study was approved by the National Research Ethics Service Committee West Midlands—Coventry & Warwickshire (project number 13/WM/0368) and registered at clinicaltrials.gov (NCT02095873). The procedures followed were in accordance

with institutional guidelines and the Declaration of Helsinki. Three participants failed to complete the study.

Main inclusion criteria were age 18–80 years, BMI 25–40 kg/m^2, and normal, impaired fasting, or impaired postprandial glucose. Main exclusion criteria were severe hypertriglyceridemia, uncontrolled hypertension, cardiovascular disease, relevant renal or hepatic disease, diabetes, and other relevant morbidity; severe excess alcohol consumption (>14/21 units [8g]/week for women/men), smoking, pharmacological treatment affecting glucose and lipid metabolism or blood coagulation, taking herbal remedies, known food allergies, pregnancy, and breast-feeding. All subjects were evenly randomized in tRES-HESP and placebo arms (n = 16) by the Clinical Trials Unit, University of Warwick. Treatment was one capsule daily for 8 weeks and a washout period of 6 weeks—tRES-HESP (90 mg tRES and 120 mg HESP) and placebo—with starch in place of bioactives in hard gelatin capsules. Previous studies with dietary fiber supplementation indicated intervention for at least 8 weeks is required for improved glycemic control (11). Participants were advised to maintain their usual diet, confirmed by dietary questionnaires at the start and end of dosing periods, and physical activity, supported by nurse and dietitian contact throughout the study.

Primary clinical end points were metabolic health (oral glucose insulin sensitivity [OGIS] index in an oral glucose tolerance test [OGTT] [75 g glucose; participants instructed to eat carbohydrate-rich diet, >150 g/day, for at least 3 days before the test, followed by an overnight fast]) (12) and vascular health (brachial artery flow-mediated dilatation [FMD], including dilatation response to a subtherapeutic dose [25 μg] of glyceryl nitrate [GTND]) (13). OGTT and FMD/GTND assessments were performed at the start and end of each treatment period between 8:00 A.M. and 10:00 A.M. in a quiet temperature-controlled room maintained at 23 ± 1°C. Markers of vascular inflammation were also assessed by commercial ELISA.

Venous blood samples were also drawn in the fasting state prior to the OGTT. Safety assessment of tRES-HESP coformulation was assessed by electrocardiogram and analysis of blood markers. Plasma methylglyoxal and glycation and oxidation adducts in plasma protein and urine (second void after overnight fast) were assayed by stable isotopic dilution analysis liquid chromatography–tandem mass spectrometry (LC-MS/MS) (14,15).

Total tRES and HESP Urinary Metabolites

Total tRES and HESP urinary metabolites were determined by stable isotopic LC-MS/MS after deconjugation of glucuronides and sulfates. Urine (20 μL), from which cells had been sedimented and removed prior to storage, with 42 mmol/L ammonium acetate buffer, pH 4.9 (60 μL), internal standards (250 μmol/L [$^{13}C_6$]tRES and 10 μmol/L d_4-HESP; 20 μL), and β-glucuronidase (5 μL, 85 units) and β-sulphatase (5 μL, 5 units), was incubated for 2 h at 37°C in the dark. Deconjugation was validated with authentic glucuronides and sulfates of tRES and HESP before use. Thereafter, ice-cold methanol (100 μL) was added for deproteinization, centrifuged (10,000g, 10 min, 4°C), and analyzed by LC-MS/MS. Calibration curves were constructed by analysis of 125–625 pmol tRES and HESP.

Cellular GSH and Oxidized Glutathione GSH–to–oxidized glutathione

Cellular GSH and oxidized glutathione (GSSG) were assayed by stable isotopic dilution analysis LC-MS/MS. Cells (~1 × 10^6 cells) were deproteinized with 10% trichloroacetic acid (40 μL) containing 0.15% NaCl and 0.25% sodium azide in water and centrifuged (20,000g, 30 min, 4°C). An aliquot of supernatant (10 μL) was mixed with 10 μL isotopic standard cocktail (100 pmol [$^{13}C_2$,^{15}N] GSH and [$^{13}C_4$,$^{15}N_2$]GSH–to–GSSG) and analyzed by LC-MS/MS. Calibration standards contained 100–2,000 pmol GSH and 5–100 pmol GSSG (Fig. 3).

Statistical Analysis

Data are mean ± SD or SEM for parametric data and median (upper–lower quartile) for nonparametric data. Significance testing in paired data was assessed by paired Student t test and Wilcoxon signed rank test (for two study groups), by ANOVA repeated measures and Friedman test (for four study groups), and by correlation analysis by Pearson and Spearman methods for parametric and nonparametric data, respectively. For HATFF study power calculation, we judged that decrease in area under the plasma glucose curve (AUCg) of the OGTT would be 10%, compared with 30% decrease with high cereal fiber intake (16). With a 30% dropout, 32 subjects were required for α = 0.05 and power (1 − β) = 0.80. Post hoc analysis of variables for highly overweight and obese subgroups was performed to explore BMI as a factor influencing responsiveness to Glo1 inducers.

RESULTS

Screening of Small-Molecule Glo1 Inducers

After screening of ~100 dietary bioactive compounds with Nrf2 activator activity, the highest maximum GLO1-ARE transcriptional activity response (E_{max}) was produced by tRES. The lowest half-maximal effective concentration (EC_{50}) for GLO1-ARE transcriptional activity was found with HESP. For tRES, EC_{50} = 2.52 ± 0.19 μmol/L and E_{max} 100 ± 2%, and for HESP, EC_{50} = 0.59 ± 0.01 μmol/L and E_{max} 24.4 ± 0.1% (Fig. 2*A* and *B*). In previous clinical studies, dietary supplementation of 150 mg HESP achieved a peak plasma concentration of 6.7 μmol/L (17), suggesting that HESP may be a competent Glo1 inducer for clinical use but with low maximal effect, and dietary supplementation of 500 mg tRES achieved a peak plasma concentration of ~0.3 μmol/L (18), eightfold lower than the EC_{50} for GLO1-ARE response. To enhance efficacy, we studied the pharmacological synergism of tRES and HESP together. Study of the GLO1-ARE transcriptional response of 5 μmol/L HESP with 0.625–10 μmol/L tRES showed that HESP combined synergistically with tRES, decreasing the EC_{50} of tRES approximately twofold to 1.46 ± 0.10 μmol/L while maintaining the E_{max} (Fig. 2*C*). The predicted increase of GLO1-ARE

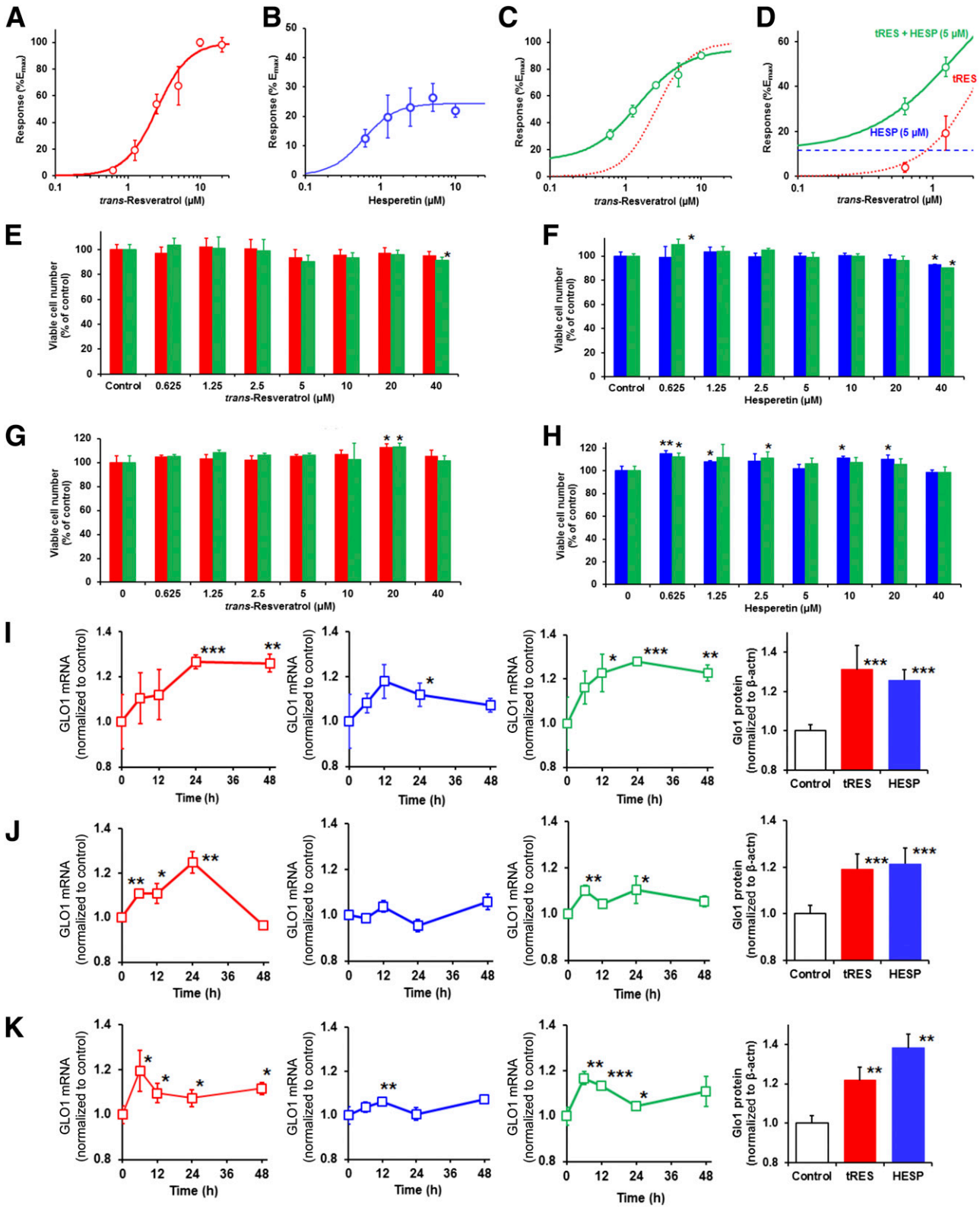

Figure 2—Induction of Glo1 expression by tRES and HESP. GLO1-ARE transcriptional response reporter assay. Data of normalized responses for varied bioactive concentrations were fitted by nonlinear regression to the equation $E = E_{max} \times [\text{bioactive}]^n/(EC_{50}{}^n + [\text{bioactive}]^n)$, solving for E_{max}, EC_{50}, and n (Hill coefficient). *A*: Concentration-response curve for tRES. Data are mean ± SD (n = 3) for 5 concentrations. Nonlinear regression (red curve): $E\ (\%) = 100 \times [\text{tRES}]^{3.92}/(2.52^{3.92} + [\text{tRES}]^{3.92})$. *B*: Concentration-response curve for HESP. Data are mean ± SD (n = 3–8) for 6 concentrations. Nonlinear regression (blue curve): $E\ (\%) = 24.4 \times [\text{HESP}]^{2.01}/(0.59^{2.01} + [\text{HESP}]^{2.01})$. *C*: Concentration-response curve for tRES in the presence of 5.0 μmol/L HESP. Data are mean ± SD (n = 3–6) for 5 concentrations. Nonlinear regression, green curve: $E\ (\%) = (83.4 \times [\text{tRES}]^{1.36}/(1.46^{1.36} + [\text{tRES}]^{1.36})) + 11.6$; green curve: tRES+ 5.0 μmol/L HESP; red dotted curve: tRES only (as for *A*). *D*: Expansion of *C*, also showing the response for 5.0 μmol/L HESP (blue dashed line).

transcriptional response from concentration response curves of 0.1–1.0 tRES in the presence of 5 μmol/L HESP was 3- to 79-fold, including up to 80% increase over additive effects (Fig. 2*D*). This suggests that marked benefits may accrue from use of tRES-HESP coformulation.

Safety assessments of tRES and HESP indicate that they are highly tolerated (19,20). Studies of human BJ fibroblasts in primary culture showed no toxicity of tRES and HESP individually or with 5 μmol/L combination with primary bioactive compound at concentrations ≤20 μmol/L. tRES (40 μmol/L) with 5 μmol/L HESP and 40 μmol/L HESP with and without 5 μmol/L tRES showed minor decrease in viability of BJ cells in vitro (Fig. 2*E* and *F*). tRES (5 μmol/L) with 0.625 μmol/L HESP gave a minor increase in cell number—possibly an effect of insulin-sensitizing activity. (See below.) There was no toxicity of tRES, HESP, or both combined in HAECs in primary culture under similar conditions (Fig. 2*G* and *H*).

Validation of Glo1 Inducer Screening Results and Functional Effects

To validate the Glo1 inducer studies, we measured the change in Glo1 mRNA and protein and functional responses in the human hepatocyte-like HepG2 cell line in vitro and HAECs and BJ fibroblasts in primary culture. There was a 10–30% increase in Glo1 mRNA in cells incubated with tRES and HESP and combined, and similar increases in Glo1 protein (Fig. 2*I–K*). We then studied the effect on functional markers: inflammatory response proteins and matrix metalloproteinase. In HAECs, treatments decreased intercellular adhesion molecule-1 (ICAM-1), receptor for advanced glycation end products (RAGE), and E-selectin protein, with synergistic effects on ICAM1 and RAGE (Fig. 3*A–C*). In BJ fibroblasts, treatments decreased cellular vascular adhesion molecule-1 (VCAM-1), RAGE, and matrix metalloproteinase-3 (MMP-3), with synergism for tRES and HESP in decrease of VCAM-1 and MMP-3 (Fig. 3*D–F*). This suggests that the tRES and HESP treatment lowers basal cell inflammation and extracellular matrix turnover.

Activation of Nrf2 is associated with increased cellular GSH and GSSG ratio through increased expression of genes of GSH synthesis and metabolism—particularly γ-glutamylcysteine ligase (modulatory and catalytic subunits [GCLM and GCLC]) and glutathione reductase. Treatment of HAECs, BJ fibroblasts, and HepG2 cells in vitro with 5 μmol/L tRES and 5 μmol/L HESP individually, however, did not change cellular levels of GSH and GSSG, whereas treatment with 5 μmol/L tRES and HESP combined increased cellular GSH content by 43% in BJ fibroblasts and 32% in HepG2 cells (Fig. 3*G–L*). Increased cellular GSH concentration enhances in situ activity of Glo1 (3).

We also studied time-dependent changes in expression of ARE-linked genes and other genes linked to metabolism and function in HAECs, BJ fibroblast, and HepG2 cells by focused quantitative mRNA array (selected time course responses are given in Supplementary Fig. 1*A–C*). Overall, there were additive and synergistic changes on gene expression of tRES and HESP combined treatment. For example, in HAECs, mRNA of ARE-linked genes glutathione transferase A4 (GTSA4), heme oxygenase-1 (HMOX-1), GCLM, GCLC, and glutathione reductase were increased. tRES and HESP together decreased ICAM1 mRNA. In BJ fibroblasts, tRES and HESP synergized to increase mRNA of GSTP1, HMOX1, NQO1, and aldoketo reductase 1C1 (AKR1C1) and to decrease expression of inflammation markers CCL2 and ICAM1. In HepG2 cells, tRES and HESP combined synergistically to increase mRNA of NQO1, GCLM, and GCLC, LDL receptor (LDLR), hexokinase-2 (HK2), and 6-phosphofructokinase/bisphosphatase-3 (PFKBP3).

Improved Clinical Metabolic and Vascular Health With tRES-HESP Coformulation: HATFF Study

Coformulation of tRES-HESP was evaluated in healthy overweight and obese subjects. Twenty-nine subjects completed the study. Characteristics of subjects at study entry are given in Table 1. Subjects had mildly impaired glycemic control, with only 9 subjects meeting criteria of prediabetes; all participants were overweight or obese, 20 were highly overweight (BMI >27.5 kg/m^2), and 11 were obese (BMI >30 kg/m^2). tRES-HESP treatment increased urinary excretion of tRES and HESP metabolites by >2,000-fold and >100-fold, respectively, compared with placebo (Supplementary Fig. 2*A* and *B*). Dietary questionnaires, urinary excretion of pyrraline—an advanced glycation end product sourced only from food (21), and fasting plasma ketone body concentrations in the normal range in all subjects (22) suggested that food consumption was similar throughout the study (Table 2). Clinical safety indicators were normal at study entry and remained unchanged throughout the placebo and tRES-HESP treatment periods (Supplementary Table 1).

E–H: Evaluation of the effect of tRES and HESP individually and in combination on the growth and viability of BJ fibroblasts (*E* and *F*) and HAECs (*G* and *H*) in vitro. For *E* and *G*, cells were incubated with 0.625–40 μmol/L tRES and with (green bars) or without (red bars) 5.0 μmol/L HESP. For *F* and *H*, cells were incubated with 0.625–40 μmol/L HESP and with (green bars) or without (blue bars) 5.0 μmol/L tRES. *I–K*: Validation of induction of Glo1 expression by 5.0 μmol/L tRES and HESP, individually and combined. Cell type: HAECs (*I*), BJ fibroblasts (*J*), and HepG2 (*K*) cells. Panels (from left to right): GLO1 mRNA change with 5.0 μmol/L tRES (red line), 5.0 μmol/L HESP (blue line), and 5.0 μmol/L tRES and HESP (green line). Bar chart: Glo1 protein (16 h posttreatment) plus 5.0 μmol/L tRES (red bar) and 5.0 μmol/L HESP (blue bar). Data are mean ± SD (n = 3) for *E–K*. Significance: *P < 0.05, **P < 0.01, and ***P < 0.001. HAEC cells were grown in proprietary large-vessel endothelial cell basal media supplemented with large-vessel endothelial cell growth supplement (containing hydrocortisone, human epidermal growth factor, and human fibroblast growth factor with heparin and in 2% [v/v] FBS), 25 μg/mL gentamicin, and 50 ng/mL amphotericin B. They were cultured in minimum essential medium with 10% FCS and 2 mmol/L glutamine under an atmosphere of 5% CO_2 in air, 100% humidity, and 37°C.

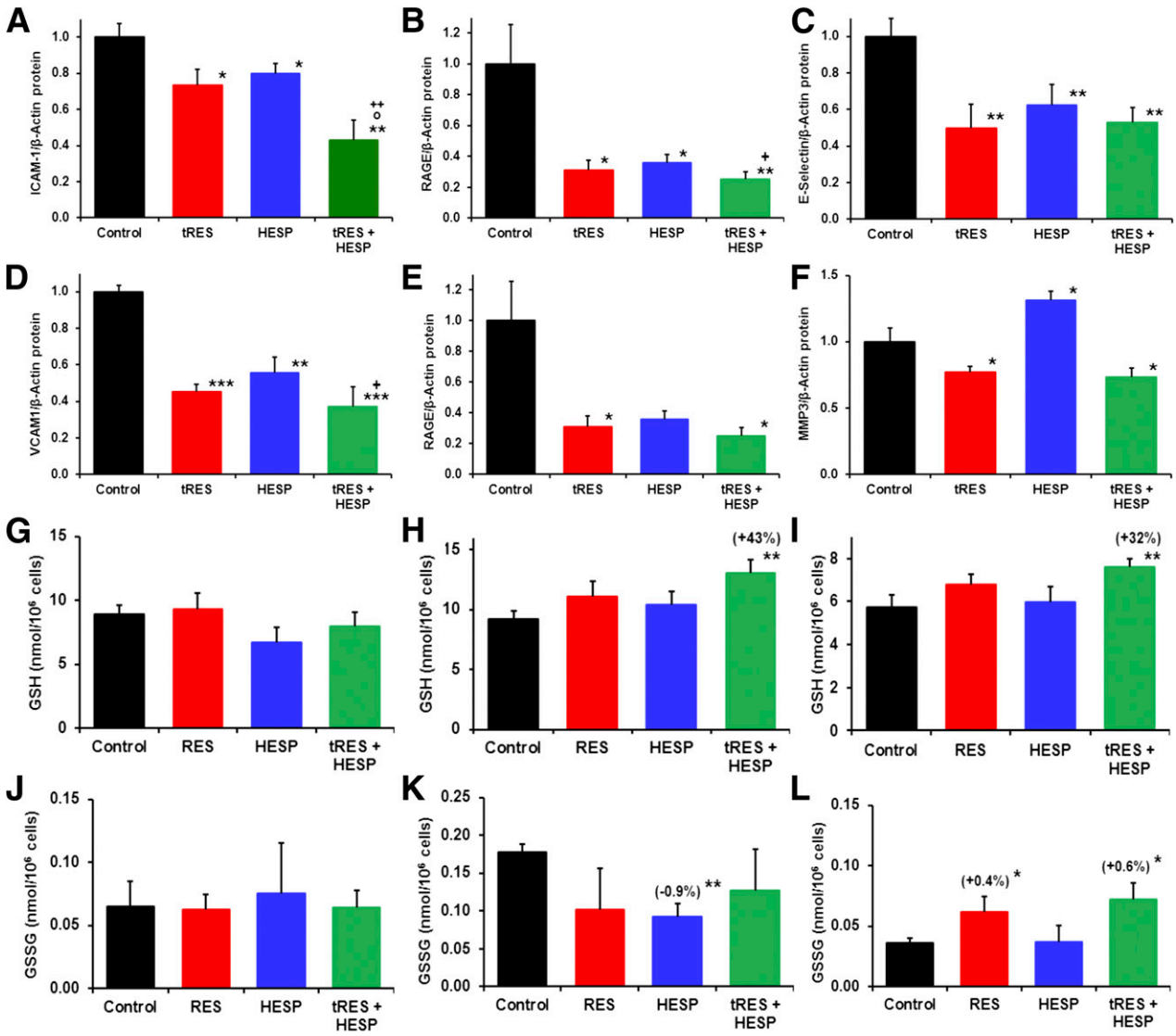

Figure 3—Effect of tRES, HESP, and tRES-HESP coaddition on cell vitality markers and glutathione metabolism in human endothelial cells, fibroblasts, and HepG2 cells in vitro. *A–F*: Cell vitality markers. Control, 5.0 μmol/L tRES, 5.0 μmol/L HESP, and 5.0 μmol/L tRES-HESP. HAECs: ICAM-1 protein (*A*) and RAGE protein (*B*) at 18 h posttreatment and E-selectin protein (*C*) and VCAM-1 protein (*D*) at 24 h posttreatment. BJ fibroblasts: RAGE protein (*E*) and MMP3 protein (*F*) at 72 h posttreatment. *G–L*: Cellular GSH and GSSG at 24 h posttreatment. GSH (*G–I*) and GSSG (*J–L*) in HAECs, BJ fibroblasts, and HepG2 cells. Percentage change with respect to GSH of control cultures is indicated. Data are mean ± SD ($n = 3$). Significance: $^{*}P < 0.05$, $^{**}P < 0.01$, and $^{***}P < 0.001$ with respect to control; $^{o}P < 0.05$ with respect to tRES control; and $^{+}P < 0.05$ and $^{++}P < 0.01$ with respect to HESP control. LC-MS/MS was performed using two Hypercarb HPLC columns in series (50 × 2.1 mm and 250 × 2.1 mm, particle size 5 μm) at temperature of 30°C. Initial mobile phase was 0.1% trifluoroacetic acid in water and the elution profile was 1–15 min, a linear gradient of 0–30% acetonitrile, and 15–16 min, isocratic 30% acetonitrile; the flow rate was 0.2 mL/min and diverted into the mass spectrometer from 4 to 16 min. Mass spectrometric analysis was performed using electrospray positive ionization mode with the following detection settings: capillary voltage 3.4 kV, source and desolvation gas temperatures 120°C and 350°C, respectively; and cone and desolvation gas flows 146 and 550 L/h, respectively. For analyte detection, the retention time, mass transition molecular ion>fragment ion, cone voltage, and collision energy were as follows: GSH, 11.7 min, 308.2 > 179.1 Da, 30 V, and 13 eV; [$^{13}C_2$,^{15}N]GSH, 11.7 min, 311.2 > 182.1 Da, 30 V, and 13 eV; GSSG, 14.4 min, 613.2 > 483.7 Da, 52 V, and 18 eV; and [$^{13}C_4$,$^{15}N_2$]GSSG, 14.4 min, 619.2 > 489.7 Da, 52 V, and 18 eV. For GSH and GSSG, limits of detection were 0.92 pmol and 1.46 pmol, analytical recoveries 97 ± 2% and 93 ± 6%, and intrabatch coefficients of variation 8.8% and 10.9% ($n = 6$), respectively.

tRES-HESP produced a 22% increase in Glo1 activity of peripheral blood mononuclear cells (PBMCs) posttreatment compared with placebo in all subjects. PBMC Glo1 activity was increased 27% in highly overweight/obese and 30% in obese subgroups. Concomitant with this there was a 37% decrease in plasma methylglyoxal postsupplementation with tRES-HESP but not with placebo in highly overweight/obese subjects. There was no change in plasma D-lactate concentration with tRES-HESP treatment—a surrogate indicator of flux of methylglyoxal formation (3) (Table 2). Therefore, increase of Glo1 activity by tRES-HESP in PBMCs, also expected in tissues, likely

Table 1—Characteristics of subjects in the HATFF study at entry

Age (years)	45 ± 13
Sex (male/female)	8/21
BMI (kg/m^2)	30.0 ± 3.8
Overweight/obese	18/11
FPG (mmol/L)	3.93 ± 0.57
A1C (mmol/mol)	36.2 ± 4.3
A1C (%)	5.5 ± 0.7
Prediabetes (no/yes)	20/9
GFR (mL/min)	97 ± 17
Systolic BP (mmHg)	133 ± 12
Diastolic BP (mmHg)	83 ± 10
Hypertension (no/yes)	18/11

Data are mean ± SD or number of each classification (class 1/class 2) unless otherwise indicated; n = 29. Hypertension was defined as systolic blood pressure (BP) ≥140 mmHg or diastolic blood pressure ≥90 mmHg on 4 occasions. Thirty-two subjects were recruited at the University Hospitals of Coventry and Warwickshire National Health Service Trust in the period May–July 2014; the last participant left the study December 2014. At prescreening, assessments made were 2-h plasma glucose in an OGTT and A1C, aspartate transaminase, alanine transaminase, plasma triglycerides, and plasma creatinine (for estimated glomerular filtration rate [GFR]). One participant was withdrawn from the study for diverging from the protocol, and 2 dropped out: 1 while on placebo and 1 on treatment. The 2 participants who dropped out stated personal reasons related to interfering duties and therefore difficulties attending the scheduled follow-up appointments. None of the participants reported any relevant side effects (nausea, loss of appetite, gastrointestinal side effects, or other symptoms). Study data were analyzed per protocol (n = 29).

decreased plasma methylglyoxal concentration without change in flux of methylglyoxal formation.

With tRES-HESP treatment, there was a positive correlation of change in OGIS from baseline (ΔOGIS) with BMI (r = 0.45, $P < 0.05$) (Fig. 4*A*). No similar correlation occurred with placebo. In the subset of highly overweight subjects, there was an increase in OGIS from baseline with tRES-HESP (ΔOGIS = 42 mL · min^{-1} · m^{-2}) (Table 2 and Fig. 4*B*) but not with placebo. This effect was further enhanced in obese subjects only (ΔOGIS = 58 mL · min^{-1} · m^{-2}) (Table 2). The main contributory factors to this effect were: *1*) decreased fasting plasma glucose (FPG) ($P < 0.01$) and *2*) decreased AUCg ($P < 0.03$, ANOVA) (Table 2).

There was a negative correlation of change in FPG from baseline (ΔFPG) to BMI with tRES-HESP treatment (r = −0.41, $P < 0.05$) (Fig. 4*C*). No similar correlation occurred with placebo. In highly overweight subjects, there was a 5% decrease in FPG postsupplementation with tRES-HESP (Fig. 4*D*). This effect was further enhanced in obese subjects only (−9%) (Table 2). There was also decreased AUCg in the OGTT with tRES-HESP treatment in the highly overweight study group to a similar extent (−8%; $P < 0.03$, ANOVA) (Table 2). Therefore, tRES-HESP treatment would likely decrease exposure to increase glucose concentration in the fasting and postprandial states in the highly overweight and obese populations.

Concomitant with increased metabolic health there were small decreases in BMI and body weight in the obese subjects with tRES-HESP: −0.5 kg/m^2 and −0.3 kg, respectively. Measurement at morning study visits excluded effect of diurnal variation. Other small changes were 3% increase in estimated glomerular filtration rate and 9% decrease in plasma urea with tRES-HESP. Further clinical variables unchanged by tRES-HESP treatment are given in Table 2.

In assessment of vascular function, we found no change in FMD or GTND. For FMD-to-GTND ratio, normalizing from baseline, in the highly overweight/obese subject group, the 95% CI for ΔFMD/ΔGTND with tRES-HESP was 0.13–2.11. Assessment of markers of vascular inflammation revealed a decrease in change of soluble intercellular adhesion molecule-1 (sICAM-1) from baseline with tRES-HESP in all subjects compared with increase with placebo: −3.6 ± 6.9 vs. 25.8 ± 6.9 ng/mL ($P < 0.01$), a reversal of ∼10% of postsupplementation placebo level.

To assess the effect on protein glycation in the HATFF study, we analyzed glycation and oxidative damage of plasma protein. Plasma protein MG-H1 was unchanged with tRES-HESP treatment (Table 1). We propose that this unexpected finding may be due to improved vascular function with tRES-HESP treatment, decreasing transcapillary escape rate of albumin (23) and increasing vascular half-life of albumin and thereby maintaining methylglyoxal plasma protein glycation. The increase of transcapillary escape rate of albumin in obesity was 36% (24)—a magnitude similar to that of the decrease of plasma methylglyoxal herein with tRES-HESP. The oxidative cross-link dityrosine was decreased 21% with tRES-HESP treatment but not with placebo (Table 2 and Fig. 4*E*). To assess the whole-body formation of MG-H1, we measured the urinary excretion of MG-H1 free adduct, corrected for MG-H1 absorbed from food by extrapolating regression of urinary MG-H1 on urinary pyrraline in all subjects to zero pyrraline (and hence no contribution from food) (25,26) (Fig. 4*F*). The flux of endogenously generated MG-H1 adducts was ∼13 nmol/mg creatinine at baseline and decreased by 14% with tRES-HESP treatment but not with placebo (Table 2 and Fig. 4*G*). The pentose-derived cross-link, pentosidine, is a quantitatively minor and fluorescent glycation adduct. Urinary excretion of pentosidine free adduct was decreased 32% by treatment with tRES-HESP but not by placebo (Fig. 4*H*).

We analyzed changes in gene expression of PBMCs in a focused quantitative mRNA array study. In all subjects, there was increased expression of GLO1 and decreased inflammation-linked genes, IL8 and PTGS2. In obese subjects, there was also decreased expression of CCL2 and TNFA (Table 3).

DISCUSSION

Pharmaceutical doses of two dietary compounds—tRES, found in red grapes, and HESP, closely related to hesperidin,

Table 2—Improvement of metabolic health with tRES-HESP coformulation in the HATFF study

Variable	Study group	Placebo		tRES-HESP		Δ + tRES-HESP from: baseline [postsupplement]	Significance *P* from: baseline [postsupplement]	ANOVA/ Friedman
		Baseline	Postsupplement	Baseline	Postsupplement			
Urinary pyrraline (nmol/mg creatinine)	All	12.1 (6.4–15.8)	10.6 (7.8–15.0)	8.8 (5.1–13.4)	8.2 (5.1– 21.3)			
PBMC Glo1 activity (mU/mg protein)	All	1,300 ± 136	1,155 ± 151	1,343 ± 156	1,414 ± 150	— [259 (22%)]	— [<0.05]	<0.02
	Highly overweight	1,346 ± 154	1,156 ± 185	1,345 ± 189	1,463 ± 177	— [307 (27%)]	— [<0.05]	<0.02
	Obese	1,451 ± 242	1,085 ± 253	1,140 ± 246	1,413 ± 264	— [328 (30%)]	— [<0.05]	
Plasma methylglyoxal (nmol/L)	Highly overweight	166 ± 28	228 ± 30	160 ± 29	133 ± 18	— [−84 (−37%)]	— [<0.05]	
Plasma D-lactate (μmol/L)	All	8.28 ± 0.81	8.56 ± 0.73	7.46 ± 0.77	8.31 ± 0.73			
OGIS (mL · min^{-1} · m^{-2})	Highly overweight	513 ± 23	541 ± 21	506 ± 22	548 ± 23	42 (8%) [—]	<0.02 [—]	<0.05
	Obese	488 ± 32	522 ± 32	489 ± 29	547 ± 30	58 (12%) [—]	<0.02 [—]	
Fasting plasma insulin (pmol/L)	All	39.6 ± 6.3	38.2 ± 5.2	43.1 ± 6.9	36.0 ± 3.2			
OGTT 90-min plasma insulin (pmol/L)	Highly overweight	291 (142–487)	326 (223–422)	303 (177–508)	240 (110–452)			
FPG (mmol/L)	Highly overweight	3.92 ± 0.12	3.80 ± 0.13	4.02 ± 0.15	3.82 ± 0.16	−0.20 (−5%) [—]	<0.04 [—]	<0.01
	Obese	3.76 ± 0.11	3.80 ± 0.16	3.92 ± 0.16	3.58 ± 0.16	−0.34 (−9%) [—]	<0.02 [—]	<0.05
AUCg (mmol/L · h)	Highly overweight	11.0 ± 0.7	10.5 ± 0.6	10.8 ± 0.7	9.9 ± 0.6	−0.9 (−8%) [—]	0.052 [—]	<0.03
BMI (kg/m^2)	Obese	34.2 ± 0.7	34.3 ± 0.6	34.0 ± 0.7	33.8 ± 0.6	— [−0.5 (−1%)]	— [<0.05]	<0.02
Body weight (kg)	Obese	93.2 (84.0–109.4)	93.6 (84.1–108.8)	93.8 (83.7–106.6)	93.3 (83.2 –107.7)	— [−0.3 (−0.3%)]	— [<0.05]	
eGFR (mL/min)	All	99 ± 2	101 ± 2	97 ± 2	100 ± 2	3 (3%) [—]	<0.03 [—]	<0.02
Plasma urea (mmol/L)	All	4.60 ± 0.19	4.35 ± 0.18	4.67 ± 0.17	4.23 ± 0.15	−0.44 (−9%) [—]	<0.01 [—]	<0.01
Plasma acetoacetate (μmol/L)	All	61 (42–135)	74 (49–113)	62 (48–127)	77 (65–125)			
Plasma β-hydroxybutyrate (μmol/L)	All	27 (16–47)	24 (13–46)	26(18–49)	22 (11–46)			
A1C (mmol/mol)	All	36.7 ± 0.8	36.5 ± 0.8	36.8 ± 0.8	36.5 ± 0.9			
A1C (%)		5.5 ± 0.1	5.5 ± 0.1	5.5 ± 0.1	5.5 ± 0.1			
OGTT 2-h glucose (mmol/L)	All	4.28 ± 0.32	4.20 ± 0.26	4.40 ± 0.29	4.40 ± 0.26			
HOMA-IR (mmol/L × mU/L)	All	0.75 (0.46–1.22)	0.68 (0.42–1.25)	0.85 (0.38–1.56)	0.69 (0.49–1.34)			

Continued on p. 2290

Table 2—Continued

Variable	Study group	Placebo		tRES-HESP		Δ + tRES-HESP from: baseline [postsupplement]	Significance *P* from: baseline [postsupplement]	ANOVA/ Friedman
		Baseline	Postsupplement	Baseline	Postsupplement			
Systolic BP (mmHg)	All	131 ± 2	132 ± 3	131 ± 3	133 ± 3			
Diastolic BP (mmHg)	All	81.7 ± 1.9	82.9 ± 2.3	83.4 ± 2.1	83.3 ± 2.3			
Total cholesterol (mmol/L)	All	5.48 ± 0.39	5.72 ± 0.28	5.35 ± 0.31	5.53 ± 0.28			
LDL/VLDL cholesterol (mmol/L)	All	3.93 ± 0.26	4.16 ± 0.23	4.01 ± 0.23	4.06 ± 0.23			
HDL cholesterol (mmol/L)	All	1.36 ± 0.10	1.39 ± 0.11	1.36 ± 0.10	1.37 ± 0.11			
Triglycerides (mmol/L)	All	0.810 ± 0.132	0.719 ± 0.122	0.650 ± 0.110	0.655 ± 0.092			
Endothelin-1 (pg/mL)	All	1.66 ± 0.17	1.61 ± 0.14	1.66 ± 0.12	1.64 ± 0.15			
CRP (μg/mL)	All	2.32 (0.99–5.46)	2.37 (0.63–3.75)	2.23 (0.82–3.97)	1.74 (0.76–3.91)			
sE-selectin (mg/mL)	All	39.0 ± 2.9	38.8 ± 3.2	39.2 ± 3.0	38.3 ± 3.0			
sVCAM1 (ng/mL)	All	453 ± 16	449 ± 13	437 ± 12	445 ± 14			
Cystatin-c (ng/mL)	All	676 ± 28	678 ± 29	692 ± 32	691 ± 31			
Albumin-to-creatinine ratio (mg albumin/mmol creatinine)	All	0.257 (0.171–0.483)	0.261 (0.147–0.790)	0.231 (0.150–0.465)	0.264 (0.159–0.581)			
FMD (mm)	All	0.18 (0.07–0.49)	0.26 (0.07–0.47)	0.17 (0.10–0.35)	0.12 (0.06–0.31)			
GTND (mm)	All	0.41 (0.36–0.77)	0.44 (0.28–0.76)	0.45 (0.37– 0.75)	0.38 (0.29– 0.53)			
Plasma sICAM-1	All	257 ± 13	284 ± 15	280 ± 13	276 ± 13			<0.01
Plasma protein MG-H1 (mmol/mol Arg)	All	0.370 (0.348–0.447)	0.380 (0.340–0.420)	0.357 (0.330–0.408)	0.381 (0.353–0.416)			
Plasma protein dityrosine (μmol/mol Tyr)	All	28.6 ± 2.7	26.6 ± 2.6	29.6 ± 2.9	23.5 ± 1.7	−6.1 (−21%) [—]	<0.01 [—]	<0.02
Total urinary MG-H1 free adduct (nmol/mg creatinine)	All	20.1 (16.3–30.6)	22.7 (16.6–29.3)	19.7 (12.5–30.4)	19.8 (14.9–27.4)			
Endogenous urinary MG-H1 free adduct (nmol/mg creatinine)	All	13.4 ± 2.1	13.5 ± 3.7	13.1 ± 2.8	11.3 ± 3.1	−1.8 (−14%) [—]	<0.01 (<0.01)	<0.01
Urinary pentosidine free adduct (pmol/mg creatinine)	All	10.8 (6.8–20.2)	12.7 (5.7–23.6)	10.8 (7.4–21.8)	7.4 (4.3–16.5)	−3.4 (−32%) [—]	<0.05 [—]	

Data are mean ± SEM or median (lower–upper quartile) unless otherwise indicated. For obese, highly overweight/obese, and all study groups, $n = 11$, 20, and 29, respectively. Variables failing to achieve or approach significance are given in Supplementary Table 1. tRES-HESP treatment changes, Δ + tRES-HESP, are absolute (percentage) changes from baseline, and changes with respect to postsupplement placebo control are in square brackets. Related significance levels are also given where $P < 0.05$ and, in one case, borderline failure of significance, $P = 0.052$. There were not statistically significant differences induced by placebo. BP, blood pressure; eGFP, estimated glomerular filtration rate; sE-selectin, soluble E-selectin.

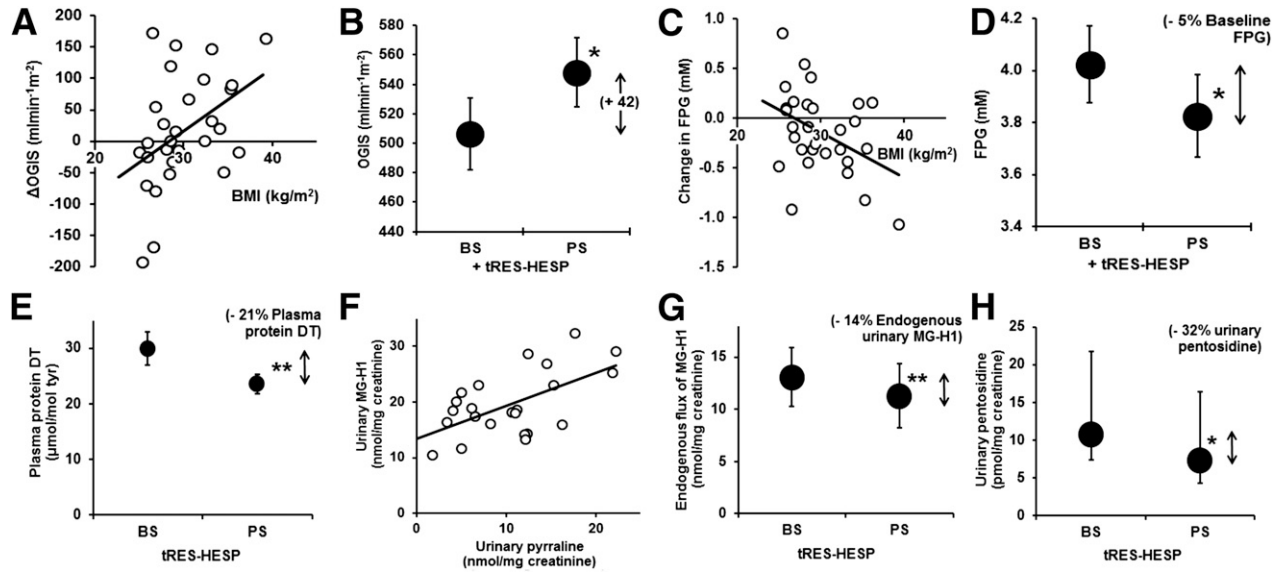

Figure 4—Outcomes from the HATFF clinical study. *A*: Correlation of change in OGIS from baseline (ΔOGIS) with BMI in the tRES-HESP treatment arm. $r = 0.45$, $P < 0.05$ (Pearson); $n = 29$. *B*: OGIS in tRES-HESP treatment arm at baseline (BS) and postsupplementation (PS) study visits in highly overweight subjects; $n = 20$. OGIS was calculated from plasma glucose concentrations at 0, 90, and 120 min and plasma insulin concentrations at 0 and 90 min (12). *C*: Correlation of change in FPG from baseline with BMI in the tRES-HESP treatment arm. $r = -0.41$, $P < 0.05$ Pearson; $n = 29$. *D*: FPG in tRES-HESP treatment arm at baseline and postsupplementation study visits in highly overweight; $n = 20$. *E*: Dityrosine residues in plasma protein at baseline and postsupplementation study visits; $n = 29$. *F*: Regression of urinary excretion of MG-H1 free adduct on urinary excretion of pyrraline free adduct at baseline of the placebo arm. Regression line: urinary MG-H1 (nmol/mg creatinine) = (0.592 ± 0.180) × urinary pyrraline (nmol/mg creatinine) + (13.4 ± 2.1); $P = 0.003$. Total urinary excretion of MG-H1 free adduct correlated positively with urinary pyrraline for all 4 study visits, $r = 0.43 – 0.63$, $P = 0.019$ to <0.001. *G*: Endogenous flux of MG-H1 formation at study visits. *H*: Urinary excretion of pentosidine free adduct at study visits. Significance: $^*P < 0.05$ and $^{**}P < 0.01$. *B*, *D*, *E*, and *G*: paired *t* test; *H:* Wilcoxon signed rank test.

found in oranges—administered together acted synergistically to improve FPG, AUCg, OGIS, sICAM-1, arterial function, and renal function in highly overweight subjects. Most clinical effects were found in the highly overweight subgroup (BMI >27.5 kg/m^2), indicating that the tRES-HESP coformulation has decreasing potency as the lean range of BMI is approached. This suggests a resetting to good metabolic and vascular health.

tRES and HESP administered individually in previous studies were ineffective. From meta-analysis, it was concluded that tRES does not affect glycemic status in overweight and obese human subjects (27). This is at odds with evidence from rodent models (28) and is likely due to interspecies differences in pharmacology, host interactions, and maximum tolerable dose. HESP absorbed from clinical dosing with hesperidin did not improve plasma glucose or insulin resistance (29).

We arrived at the tRES-HESP formulation through maximizing induction of Glo1 expression. While increased Glo1 expression likely contributes to the observed beneficial health effects (3), changes in other gene expression occurred—such as induction of antioxidant enzymes and GSH synthesis (Fig. 3*H* and *I* and Supplementary Fig. 1), and their interplay may also mediate the overall health benefit achieved. We exploited the regulatory ARE of GLO1 to increase expression (6). We limited the small-molecule inducer screen to nontoxic dietary bioactive compounds of known or suspected Nrf2 activation activity to provide an option for use of Glo1 inducers as functional food supplements as well as pharmaceuticals. tRES and HESP also have a >50-fold safety margin

Table 3—Summary of change in gene expression of PBMC with tRES-HESP coformulation in the HATFF study

		Genes	
Study group	*n*	Increased	Decreased
All	29	GLO1 (6%)	HIF1A (−6%), IL8 (−39%), and PTGS2 (−30%)
Highly overweight/obese	20		FTH1 (−19%), HIF1A (−8%), IL8 (−49%), PTGS2 (−31%), RAGE (−37%), and CCL2 (−49%)
Obese	11		CCL2 (−22%), HIF1A (−7%), IL8 (−62%), KEAP1 (−18%), PTGS2 (−37%), and TNFA (−12%)

Data and statistical analysis are given in Supplementary Table 2.

at doses used in the HATFF study (19,20). Activation of Nrf2 by dietary bioactive compounds is mostly studied through ARE-linked induction of NQO1 or HMOX1 expression. Small-molecule activators of Nrf2 increase expression of different ARE-linked gene subsets (6,7)—likely due to the ability of Nrf2 activators to recruit the requisite accessory proteins and increase nuclear concentration of functionally active Nrf2 to the level required for increased expression of the ARE-linked gene of interest (7,8). A specific functional screen for GLO1-ARE transcriptional activation was therefore required.

Activation of Nrf2 by tRES has been studied previously by induction of HMOX1 expression (30). Herein we found that tRES also induces expression of Glo1 with high E_{max}. Our recent studies (7,8) and those of others (31) suggest that this is achieved by preventing nuclear acetylation and inactivation of Nrf2 via increasing in situ activity of sirtuin-1. At low tRES concentrations, this occurs through inhibition of cAMP phosphodiesterases, activation of AMPK, and increased NAD^+. HESP may also synergize for increased activity of sirtuin-1 through activation of AMPK by the protein kinase A pathway (32,33).

Clinically achievable concentrations of tRES at highly tolerable doses are lower than the EC_{50} for induction of Glo1 expression, however, so synergism with HESP is required to achieve increased Glo1 expression in clinical translation. HESP may activate Nrf2 through induction and activation of protein kinase A, upstream of fyn kinase, which drives Nrf2 translocational oscillations and ARE-linked gene expression (8,33). HESP is a partial agonist (Fig. 2*B*), which is likely due to inhibitory nuclear acetylation of Nrf2 blocking a high E_{max}. Combination with tRES and HESP provides for faster nuclear translocation and decreased inactivation of Nrf2 (7,8,31). Use of HESP rather than related dietary glycoside hesperidin found in citrus fruits (34) is likely crucial: HESP has ~70-fold greater potency in Nrf2 activation and higher bioavailability than hesperidin (35).

tRES-HESP increased OGIS to levels typical of healthy, lean subjects. The magnitude of ΔOGIS, 42–58 mL · min^{-1} · m^{-2}, is comparable to that achieved with pharmaceutical treatment of patients with type 2 diabetes (for example, 1.7 g metformin per day, ΔOGIS = increase of 54 mL · min^{-1} · m^{-2}) (36) and extreme weight loss with gastric band surgery in morbid

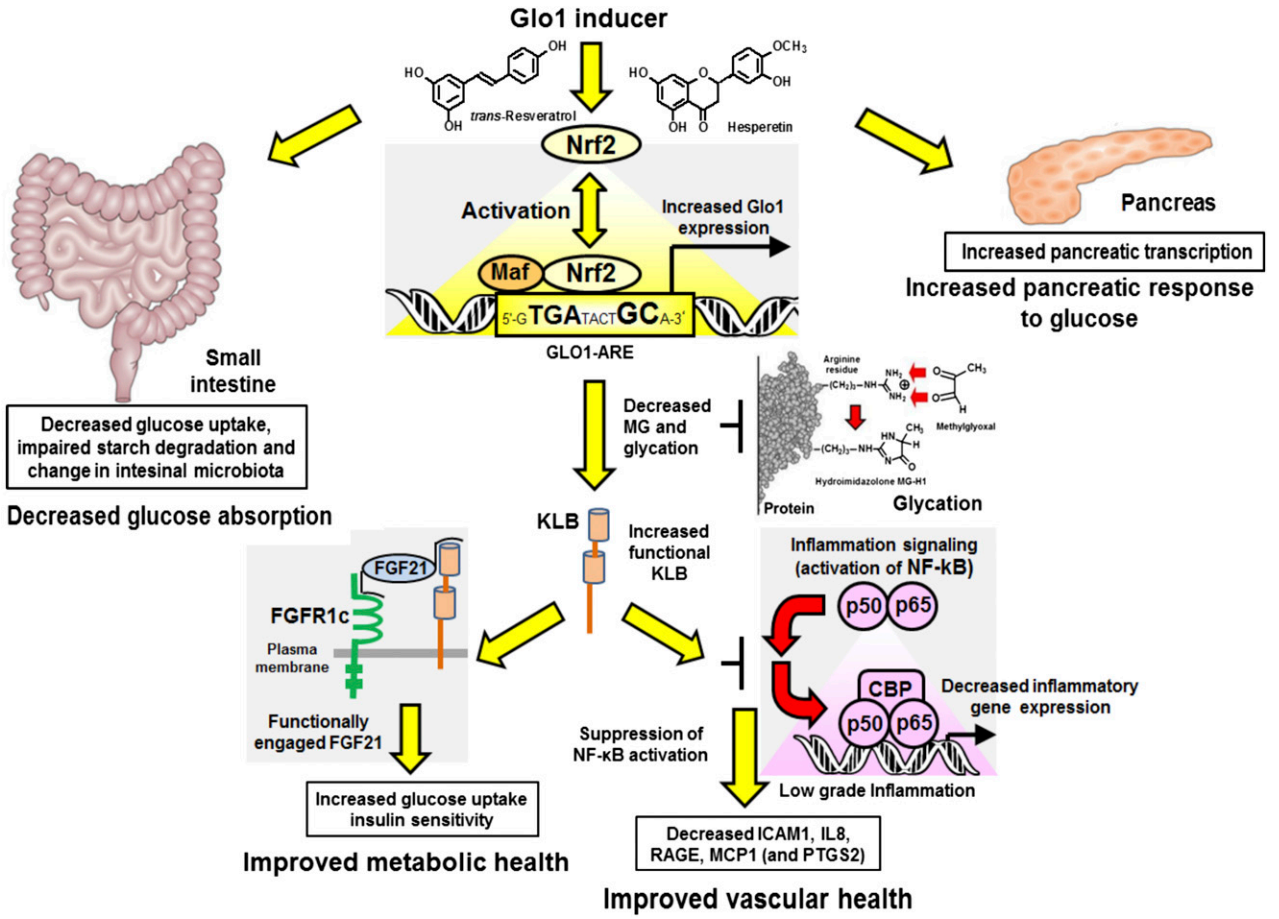

Figure 5—Proposed mechanism of action of Glo1 inducer formulation. Yellow-filled arrows, mechanism of health improvement; red-filled arrows, damaging processes suppressed. See also 40,42–44. CBP, CREB-binding protein; FGFR1c, fibroblast growth factor receptor 1c; KLB, β-Klotho; Maf, small Maf protein, an accessory protein for Nrf2 activation.

obesity (ΔOGIS = increase of 62 mL · min^{-1} · m^{-2}) (37). These effects suggest the tRES-HESP can support therapeutic improvement of insulin sensitivity in highly overweight populations. OGIS was initially proposed as a marker of insulin resistance but is also improved with increased β-cell sensitivity to glucose and decreased glucose absorption (38). Regarding insulin resistance, decreased activity of FGF21 due to downregulation of the FGF21 receptor cofactor β-Klotho may be involved (39). Methylglyoxal-driven protein glycation decreased expression of β-Klotho (40). By inducing Glo1 expression and decreasing methylglyoxal protein glycation, therefore, we likely corrected the functional deficit of β-Klotho and reengaged FGF21. This explains the resetting of insulin sensitivity to normal levels with the response greater for higher-BMI subject groups. Characteristics of increased β-Klotho was its blocking of inflammatory signaling to downregulate proinflammatory mediators IL8, MCP1, ICAM-1, and RAGE (40) and, via decreasing MCP-1, also suppressing of PTGS2 (41) (Fig. 5). All features of this transcriptional signature were found in PBMCs of the HATFF study. Other effects increasing OGIS may be increased pancreatic β-cell sensitivity to glucose (42), decreased intestinal absorption of glucose (43), changes of gut microbiota, and decreased breakdown and absorption of starch (44) (Fig. 5).

The 5% decrease in FPG herein exceeds and matches effects of metformin and Olristat, respectively, in similar intervention trials in overweight/obese subjects (45,46). Decrease in FPG in the normal range is associated with reduced risk of developing type 2 diabetes (47).

Decreased urinary excretion of pentosidine by tRES-HESP may be linked to decreased oxidative stress and decreased pentose precursors expected from improved insulin resistance (48).

tRES-HESP treatment produced an increase in ΔFMD/ΔGTND. The effect is likely produced by improved nitric oxide responsiveness in both endothelium and smooth muscle cells (13) related to induction of Glo1 and prevention of methylglyoxal glycation–driven impairment of endothelial nitric oxide synthase (49). tRES-HESP also decreased dityrosine content of plasma protein. Dityrosine is an oxidative cross-link of tyrosine residues and is a dominant cross-link of the extracellular matrix (50). Plasma protein dityrosine may be a surrogate marker of this and hence be reporting decreased dityrosine cross-linking, which may contribute to improved arterial function.

tRES-HESP decreased sICAM-1 in the HATFF study. The cell studies herein suggest that this is likely linked to decreased ICAM-1 expression. ICAM-1 expression was decreased in Glo1 transgenic rats (51). In clinical studies, tRES and HESP individually did not decrease ICAM1 (52,53). sICAM-1 correlates with atherosclerosis burden assessed by coronary artery calcification and is a risk predictor of cardiovascular disease (54).

In summary, we present evidence that pharmaceutical doses of tRES and HESP coformulation produce improved metabolic and vascular health in overweight and obese subjects.

Acknowledgments. The authors thank Louise Goodbody, supporting research nurse, and Louise Halder, research dietician, in the HATFF study. A.S. thanks Taif University, the Ministry of Education, Government of Saudi Arabia, for a PhD studentship.

Duality of Interest. This research was mainly funded by Unilever and Innovate UK (project no. 101129). D.M., M.F., and G.J. are employees of Unilever. No other potential conflicts of interest relevant to this article were reported.

Author Contributions. M.X. performed screening, validation, and most clinical chemistry analysis. M.O.W. was clinical lead and codesigned and analyzed data of the HATFF study. S.Q. performed the clinical procedures. N.-B.K. was the HATFF study statistician. A.A. and A.S. performed some clinical chemistry analysis. M.W. was the principal HATFF study research nurse. D.M. and M.F. participated in quarterly project steering meetings. G.J. participated in quarterly project steering meetings and raised funding for the study. N.R. was study coordinator, codesigned the study, and performed some metabolite analysis. P.J.T. designed and led the study, raised funding for the study, performed some metabolite analysis, analyzed data, and wrote the manuscript. All authors read and approved the manuscript. P.J.T. is the guarantor of this work and, as such, had full access to all the data in the study and takes responsibility for the integrity of the data and the accuracy of the data analysis.

References

1. Mäkinen V-P, Civelek M, Meng Q, et al.; Coronary ARtery DIsease Genome-Wide Replication And Meta-Analysis (CARDIoGRAM) Consortium. Integrative genomics reveals novel molecular pathways and gene networks for coronary artery disease. PLoS Genet 2014;10:e1004502

2. Wilson AF, Elston RC, Tran LD, Siervogel RM. Use of the robust sib-pair method to screen for single-locus, multiple-locus, and pleiotropic effects: application to traits related to hypertension. Am J Hum Genet 1991;48:862–872

3. Rabbani N, Thornalley PJ. Dicarbonyl stress in cell and tissue dysfunction contributing to ageing and disease. Biochem Biophys Res Commun 2015;458:221–226

4. Thornalley PJ, Battah S, Ahmed N, et al. Quantitative screening of advanced glycation endproducts in cellular and extracellular proteins by tandem mass spectrometry. Biochem J 2003;375:581–592

5. Thornalley PJ, Waris S, Fleming T, et al. Imidazopurinones are markers of physiological genomic damage linked to DNA instability and glyoxalase 1-associated tumour multidrug resistance. Nucleic Acids Res 2010;38:5432–5442

6. Xue M, Rabbani N, Momiji H, et al. Transcriptional control of glyoxalase 1 by Nrf2 provides a stress-responsive defence against dicarbonyl glycation. Biochem J 2012;443:213–222

7. Xue M, Momiji H, Rabbani N, et al. Frequency modulated translocational oscillations of Nrf2 mediate the ARE cytoprotective transcriptional response. Antioxid Redox Signal 2015;23:613–629

8. Xue M, Momiji H, Rabbani N, Bretschneider T, Rand DA, Thornalley PJ. Frequency modulated translocational oscillations of Nrf2, a transcription factor functioning like a wireless sensor. Biochem Soc Trans 2015;43:669–673

9. Hansen MB, Nielsen SE, Berg K. Re-examination and further development of a precise and rapid dye method for measuring cell growth/cell kill. J Immunol Methods 1989;119:203–210

10. Fortina P, Surrey S. Digital mRNA profiling. Nat Biotechnol 2008;26:293–294

11. Whelton SP, Hyre AD, Pedersen B, Yi Y, Whelton PK, He J. Effect of dietary fiber intake on blood pressure: a meta-analysis of randomized, controlled clinical trials. J Hypertens 2005;23:475–481

12. Mari A, Pacini G, Murphy E, Ludvik B, Nolan JJ. A model-based method for assessing insulin sensitivity from the oral glucose tolerance test. Diabetes Care 2001;24:539–548

13. Black MA, Cable NT, Thijssen DHJ, Green DJ. Impact of age, sex, and exercise on brachial artery flow-mediated dilatation. Am J Physiol Heart Circ Physiol 2009;297:H1109–H1116

14. Rabbani N, Thornalley PJ. Measurement of methylglyoxal by stable isotopic dilution analysis LC-MS/MS with corroborative prediction in physiological samples. Nat Protoc 2014;9:1969–1979
15. Rabbani N, Shaheen F, Anwar A, Masania J, Thornalley PJ. Assay of methylglyoxal-derived protein and nucleotide AGEs. Biochem Soc Trans 2014;42:511–517
16. Weickert MO, Mohlig M, Koebnick C, et al. Impact of cereal fibre on glucose-regulating factors. Diabetologia 2005;48:2343–2353
17. Takumi H, Nakamura H, Simizu T, et al. Bioavailability of orally administered water-dispersible hesperetin and its effect on peripheral vasodilatation in human subjects: implication of endothelial functions of plasma conjugated metabolites. Food Funct 2012;3:389–398
18. Boocock DJ, Faust GES, Patel KR, et al. Phase I dose escalation pharmacokinetic study in healthy volunteers of resveratrol, a potential cancer chemopreventive agent. Cancer Epidemiol Biomarkers Prev 2007;16:1246–1252
19. Vang O, Ahmad N, Baile CA, et al. What is new for an old molecule? Systematic review and recommendations on the use of resveratrol. PLoS One 2011;6:e19881
20. Parhiz H, Roohbakhsh A, Soltani F, Rezaee R, Iranshahi M. Antioxidant and anti-inflammatory properties of the citrus flavonoids hesperidin and hesperetin: an updated review of their molecular mechanisms and experimental models. Phytother Res 2015;29:323–331
21. Foerster A, Henle T. Glycation in food and metabolic transit of dietary AGEs (advanced glycation end-products): studies on the urinary excretion of pyrraline. Biochem Soc Trans 2003;31:1383–1385
22. Mahendran Y, Vangipurapu J, Cederberg H, et al. Association of ketone body levels with hyperglycemia and type 2 diabetes in 9,398 Finnish men. Diabetes 2013;62:3618–3626
23. Rabbani N, Thornalley PJ. Hidden complexities in the measurement of fructosyl-lysine and advanced glycation end products for risk prediction of vascular complications of diabetes. Diabetes 2015;64:9–11
24. Parving HP, Gyntelberg F. Transcapillary escape rate of albumin and plasma volume in essential hypertension. Circ Res 1973;32:643–651
25. Ahmed N, Mirshekar-Syahkal B, Kennish L, Karachalias N, Babaei-Jadidi R, Thornalley PJ. Assay of advanced glycation endproducts in selected beverages and food by liquid chromatography with tandem mass spectrometric detection. Mol Nutr Food Res 2005;49:691–699
26. Ahmed N, Thornalley PJ, Lüthen R, et al. Processing of protein glycation, oxidation and nitrosation adducts in the liver and the effect of cirrhosis. J Hepatol 2004;41:913–919
27. Liu K, Zhou R, Wang B, Mi M-T. Effect of resveratrol on glucose control and insulin sensitivity: a meta-analysis of 11 randomized controlled trials. Am J Clin Nutr 2014;99:1510–1519
28. Baur JA, Pearson KJ, Price NL, et al. Resveratrol improves health and survival of mice on a high-calorie diet. Nature 2006;444:337–342
29. Rizza S, Muniyappa R, Iantorno M, et al. Citrus polyphenol hesperidin stimulates production of nitric oxide in endothelial cells while improving endothelial function and reducing inflammatory markers in patients with metabolic syndrome. J Clin Endocrinol Metab 2011;96:E782–E792
30. Chen C-Y, Jang J-H, Li M-H, Surh Y-J. Resveratrol upregulates heme oxygenase-1 expression via activation of NF-E2-related factor 2 in PC12 cells. Biochem Biophys Res Commun 2005;331:993–1000
31. Yang Y, Li W, Liu Y, et al. Alpha-lipoic acid improves high-fat diet-induced hepatic steatosis by modulating the transcription factors SREBP-1, FoxO1 and Nrf2 via the SIRT1/LKB1/AMPK pathway. J Nutr Biochem 2014;25:1207–1217
32. Park S-J, Ahmad F, Philp A, et al. Resveratrol ameliorates aging-related metabolic phenotypes by inhibiting cAMP phosphodiesterases. Cell 2012;148:421–433
33. Hwang S-L, Lin J-A, Shih P-H, Yeh C-T, Yen G-C. Pro-cellular survival and neuroprotection of citrus flavonoid: the actions of hesperetin in PC12 cells. Food Funct 2012;3:1082–1090
34. Chen MC, Ye YY, Ji G, Liu JW. Hesperidin upregulates heme oxygenase-1 to attenuate hydrogen peroxide-induced cell damage in hepatic L02 cells. J Agric Food Chem 2010;58:3330–3335
35. Nielsen ILF, Chee WSS, Poulsen L, et al. Bioavailability is improved by enzymatic modification of the citrus flavonoid hesperidin in humans: a randomized, double-blind, crossover trial. J Nutr 2006;136:404–408
36. Kautzky-Willer A, Tura A, Winzer C, et al. Insulin sensitivity during oral glucose tolerance test and its relations to parameters of glucose metabolism and endothelial function in type 2 diabetic subjects under metformin and thiazolidinedione. Diabetes Obes Metab 2006;8:561–567
37. Hanusch-Enserer U, Cauza E, Spak M, et al. Improvement of insulin resistance and early atherosclerosis in patients after gastric banding. Obes Res 2004;12:284–291
38. Hücking K, Watanabe RM, Stefanovski D, Bergman RN. OGTT-derived measures of insulin sensitivity are confounded by factors other than insulin sensitivity itself. Obesity (Silver Spring) 2008;16:1938–1945
39. Gallego-Escuredo JM, Gómez-Ambrosi J, Catalan V, et al. Opposite alterations in FGF21 and FGF19 levels and disturbed expression of the receptor machinery for endocrine FGFs in obese patients. Int J Obes 2015;39:121–129
40. Zhao Y, Banerjee S, Dey N, et al. Klotho depletion contributes to increased inflammation in kidney of the db/db mouse model of diabetes via RelA (serine) 536 phosphorylation. Diabetes 2011;60:1907–1916
41. Futagami S, Hiratsuka T, Shindo T, et al. COX-2 and CCR2 induced by CD40 ligand and MCP-1 are linked to VEGF production in endothelial cells. Prostaglandins Leukot Essent Fatty Acids 2008;78:137–146
42. Fiori JL, Shin Y-K, Kim W, et al. Resveratrol prevents β-cell dedifferentiation in nonhuman primates given a high-fat/high-sugar diet. Diabetes 2013;62:3500–3513
43. Guschlbauer M, Klinger S, Burmester M, Horn J, Kulling SE, Breves G. trans-Resveratrol and ε-viniferin decrease glucose absorption in porcine jejunum and ileum in vitro. Comp Biochem Physiol A Mol Integr Physiol 2013;165:313–318
44. Unno T, Hisada T, Takahashi S. Hesperetin modifies the composition of fecal microbiota and increases cecal levels of short-chain fatty acids in rats. J Agric Food Chem 2015;63:7952–7957
45. Park MH, Kinra S, Ward KJ, White B, Viner RM. Metformin for obesity in children and adolescents: a systematic review. Diabetes Care 2009;32:1743–1745
46. Mancini MC, Halpern A. Orlistat in the prevention of diabetes in the obese patient. Vasc Health Risk Manag 2008;4:325–336
47. Tirosh A, Shai I, Tekes-Manova D, et al.; Israeli Diabetes Research Group. Normal fasting plasma glucose levels and type 2 diabetes in young men. N Engl J Med 2005;353:1454–1462
48. Wang F, Zhao Y, Niu Y, et al. Activated glucose-6-phosphate dehydrogenase is associated with insulin resistance by upregulating pentose and pentosidine in diet-induced obesity of rats. Horm Metab Res 2012;44:938–942
49. Jo-Watanabe A, Ohse T, Nishimatsu H, et al. Glyoxalase I reduces glycative and oxidative stress and prevents age-related endothelial dysfunction through modulation of endothelial nitric oxide synthase phosphorylation. Aging Cell 2014;13:519–528
50. Edens WA, Sharling L, Cheng G, et al. Tyrosine cross-linking of extracellular matrix is catalyzed by Duox, a multidomain oxidase/peroxidase with homology to the phagocyte oxidase subunit gp91phox. J Cell Biol 2001;154:879–891
51. Brouwers O, Niessen PMG, Miyata T, et al. Glyoxalase-1 overexpression reduces endothelial dysfunction and attenuates early renal impairment in a rat model of diabetes. Diabetologia 2014;57:224–235
52. van der Made SM, Plat J, Mensink RP. Resveratrol does not influence metabolic risk markers related to cardiovascular health in overweight and slightly obese subjects: a randomized, placebo-controlled crossover trial. PLoS One 2015;10:e0118393
53. Morand C, Dubray C, Milenkovic D, et al. Hesperidin contributes to the vascular protective effects of orange juice: a randomized crossover study in healthy volunteers. Am J Clin Nutr 2011;93:73–80
54. Tang W, Pankow JS, Carr JJ, et al. Association of sICAM-1 and MCP-1 with coronary artery calcification in families enriched for coronary heart disease or hypertension: the NHLBI Family Heart Study. BMC Cardiovasc Disord 2007;7:30